



Research Article

An Experimental Testing of Optimized Fuzzy Logic-Based MPPT for a Standalone PV System Using Genetic Algorithms

**Fatah Yahiaoui,¹ Ferhat Chabour,² Ouahib Guenounou,¹ Mohit Bajaj,^{3,4,5}
Syed Sabir Hussain Bukhari,⁶ Muhammad Shahzad Nazir ,⁷ Mukesh Pushkarna,⁸
and Daniel Eutyche Mbadjoun Wapet ⁹**

¹Laboratoire de Technologie Industrielle et de l'Information (LTII), Faculté de Technologie, Université de Béjaïa, Béjaïa 06000, Algeria

²GREAH Laboratory, University of Le Havre, 25 Rue Philippe Lebon, Le Havre 76600, France

³Department of Electrical Engineering, Graphic Era (Deemed to be University), Dehradun 248002, India

⁴Graphic Era Hill University, Dehradun 248002, India

⁵Applied Science Research Center, Applied Science Private University, Amman 11931, Jordan

⁶School of Electrical and Electronics Engineering, Chung-Ang University, Dongjak-gu, Seoul 06974, Republic of Korea

⁷Faculty of Automation, Huaiyin Institute of Technology, Huai'an 223003, China

⁸Department of Electrical Engineering, GLA University, Mathura 281406, India

⁹National Advanced School of Engineering, Université de Yaoundé I, Yaoundé, Cameroon

Correspondence should be addressed to Daniel Eutyche Mbadjoun Wapet; eutychedan@gmail.com

Received 7 October 2022; Revised 28 December 2022; Accepted 9 April 2023; Published 27 April 2023

Academic Editor: Ardashir Mohammadzadeh

Copyright © 2023 Fatah Yahiaoui et al. This is an open access article distributed under the Creative Commons Attribution License, which permits unrestricted use, distribution, and reproduction in any medium, provided the original work is properly cited.

The choice and the dimensioning of the controller for the maximum power point tracking (MPPT) are determined for the ideal energy efficiency of the photovoltaic (PV) systems. Many works have been developed in the field of MPPT methods, especially fuzzy logic controllers. However, these are robust if the parameters of the membership functions have been well designed. In this paper, the performances of an intelligent fuzzy logic controller (FLC)-based MPPT method have been optimized by an evolutionary genetic algorithm (GA). The works presented in the literature have shown the efficiency of the proposed method compared to classical methods. In our paper, the validation of the experimental results obtained is given with respect to a reference signal. The control of the simulated PV source and the proposed method are built using the Simulink/Matlab environment and implemented on the dSPACE DS1104 controller to validate the practical execution of the suggested method. The standalone PV system has been tested in an emulated test bench experimentation. Experimental results confirm the efficiency of the proposed method and its high accuracy in handling fast varying load conditions.

1. Introduction

Renewable energy is critical to sustainable development around the globe. Photovoltaic (PV) energy is one of the most abundantly available and cost-effective renewable energy sources. PV power is utilized in grid-integrated, standalone, and hybrid energy systems [1]. Standalone PV systems are utilized in distant locations where power from the main AC grids is not available. PV systems that include an energy storage system. PV power is also integrated into

a grid using power converters, and in order to meet the standards of grid codes, the integration of such power source needs sophisticated control techniques. Hybrid power systems can be produced by combining solar photovoltaic systems with wind, tidal, and thermal energy [2]. However, due to the stochastic nature of solar/PV energy, the output power produced by PV systems is also fluctuating.

The solar panel can give the maximum amount of power to the load at its ideal operating point. Maximum power point (MPP) is the common name for the specific operating

point. Because solar irradiation and cell temperature have a significant impact on the current-voltage characteristic of PV modules, the locus of MPP exhibits nonlinear change. The MPPT is to be created for the PV system due to the nonlinearity of PV modules. At any solar irradiation and temperature, MPPT is able to determine the PV panel MPP operating voltage. The PV system controls the PV module's voltage to the MPP operating voltage. It is possible to draw as much power as you can. As a result, the PV system's effectiveness can be increased [2, 3].

Several research algorithms have been reported to extract the maximum power from solar panels under stochastic environmental conditions. A number of techniques have been presented in recent years as examples, including perturb and observe (P&O) [4], incremental conductance (INC) [5], and fuzzy logic controller (FLC) [6].

The simplest algorithms are P&O and INC. However, due to the fact that the disturbance continues even when the system is functioning at the MPP, these techniques lead to power oscillations around the MPP. The duty cycle step might be decreased to address this problem. However, in this scenario, as atmospheric circumstances change, the system will track the MPP slowly. The PV system's total efficiency is decreased as a result of the power losses. A slight change in the step size in the P&O algorithm disrupts algorithm control. The measurement of PV system output power causes a slight modification to the direction of the step size specified by the P&O technique. Common problems could occur if a PV panel's output power is increased or decreased abruptly [7].

Alternatively, the FLC is used to track an MPP with more accuracy due to its inherent advantages in handling nonlinearity and the lack of a mathematical model, but this algorithm is greatly related to user experience with the PV panel characteristics. As reported in [8], an MPPT algorithm based on the FLC has been applied successfully for a photovoltaic generator system with a variable resistive. From the presented results, the FLC-based MPPT algorithm ensured enhanced performance as compared to the P&O technique. Similarly, in [9], an FLC-based MPPT controller is tested under variable atmospheric conditions. The FLC MPPT controller proposed in [9] guaranteed the optimal operation and performance of the autonomous PV system. In [10, 11], authors reported fuzzy controllers to regulate the power generated in a hybrid system containing PV and wind turbine systems. The study of interval type-3 fuzzy logic controllers (IT3 FLCs) has gotten a lot of attention recently. Numerous studies have demonstrated that IT3 FLCs can manage uncertainties better than their type-1 (T1) and type-2 (T2) counterparts [12].

Even though FLC controllers have many advantages, building them is still challenging since there is no standardized method for locating fuzzy control rules and fine-tuning the membership function parameters of the controllers. To get the better of this limitation, the design procedures are formulated as optimization problems that are typically solved using evolutionary algorithms [13–15], such as genetic algorithms (GAs). GAs are widely regarded as one of the most effective optimization techniques. The GA is

capable of solving a wide range of complex optimization problems, including those with nonderivable cost functions [16]. Genetic algorithms attempt to simulate the evolutionary process of species in their natural environment: an artificial transposition of basic concepts of genetics and the laws of survival stated by Darwin.

A GA is constructed in quite analogous way. In the solution set of an optimization problem, a population of size N consists of N solutions (the individuals in the population) suitably marked by coding that identifies them completely. An evaluation procedure is necessary to determine the strength of each individual in the population. Then, there is a selection phase (in which individuals are chosen in proportion to their strength) and a recombination phase (in which artificial operators of crossing and mutation are used to generate a new population of individuals with a good chance of being stronger than those in the previous generation). From generation to generation, the strength of the individuals in the population increases, and after a certain number of iterations, the population is entirely composed of strong individuals, that is to say, of quasi-optimal solutions to the problem.

Theoretical work on the optimization problem of fuzzy controllers has been widely reported in the literature. A GA-based optimization problem is solved in [17] to find the optimal scaling parameters of a fuzzy logic-based MPPT controller that maximizes the efficiency of a PV pumping system. In [18], the algorithm GA is used to optimize the following two controllers: the fuzzy PI (proportional and integrator) and the P&O PI. The simulation results presented in this article have demonstrated that the fuzzy PI-GA is better than the P&O PI-GA in terms of response time. Similarly, in [19], theoretical simulations have been carried out. The authors have used a hierarchical genetic algorithm to design a fuzzy controller for the command of a photovoltaic conversion system.

The implementation aspect of optimized fuzzy controllers has been reported in [20–25]. An experimental study on the MPPT controller using the FPGA (field programmable gate array) has been presented in [21]. Based on the obtained results, the authors concluded that the optimized FLC outperforms the conventional P&O method in terms of response time and steady-state fluctuations. In [23], FPGA implementation of MPPT-based fuzzy logic is investigated for standalone PV conversion systems. In [24], FPGA implementation of a fuzzy controller is reported for a PV system. The authors in [25] discuss the MPPT technique based on GAs for a standalone PV conversion system. The results have been compared with the conventional techniques. The results have been validated experimentally using a dSPACE control board. Another two hardware implementations of fuzzy controllers for MPPT of PV systems have been described in recent works [26, 27]. The experimental results obtained have been compared to a conventional P&O method. The fuzzy controller design has been better than the P&O. However, it shows significant oscillations at the optimal point.

This paper discusses the hardware implementation of a fuzzy controller optimized by the GA algorithm for MPPT tracking using the dSPACE 1104 control board. The

proposed MPPT method is tested for maximum harvesting power under real-time environmental conditions. The following is a summary of the primary differences between the current work and the related literature:

- (i) The fuzzy controller is optimized to improve the convergence speed for maximum power harvesting of the PV system. The suggested technique can also track the global MPP (GMPP) efficiently, which is very beneficial in variable atmospheric conditions.
- (ii) The proposed algorithm is tested for fast-changing solar irradiation and a variable resistance load.
- (iii) In the cited literature [20–25], the design of a fuzzy MPPT controller using the GA optimization algorithm is accomplished for a learning profile of constant conditions ($T = 25^\circ\text{C}$ and $S = 1000 \text{ W/m}^2$). However, atmospheric conditions are constantly changing. In this work, different variations of the irradiance (600 W/m^2 , 1000 W/m^2 , and 800 W/m^2) are adopted to test the robustness of the optimized control utilized.

The paper's sections are structured as follows: Section 2 is a description of the system. Section 3 shows the design procedures of the fuzzy controller. Section 4 shows the proposed optimized control strategy. Section 5 presents the steps of the details of the experimental real-time platform. The result discussion is also presented in this section. Finally, Section 6 presents a general conclusion that will summarize the content of this work and put forward the results obtained.

2. Standalone PV System Description

Figure 1 shows a block diagram of a standalone PV system. The components of the system are the PV panel connected to a variable resistive load through a matching stage. The latter is composed of a boost converter. The switch of the converter is controlled by the signals generated by the proposed method.

2.1. PV Panel Model's Mathematical Equation. There are a few different sorts of models, such as single-diode and two-diode models [28, 29]. The two-diode model accounts for a second diode that is wired in parallel with the first diode in the circuit that functions as a single diode's equivalent. Compared to a two-diode model, the one-diode model has fewer parameters and is simpler to model. The electrical properties $P(V)$ and $I(V)$ of the solar panel as simulated and experimental data clearly demonstrate that the results are identical, according to the paper [29]. The one-diode model of the solar cell is used in this paper [29].

The PV panel model's mathematical equation is formulated according to the cell's number in series only, and the cell's number in parallel is equal to 1 according to our BP SX150S model in the following equation:

$$I_{pv} = I_{ph} - I_s \left(\exp \left(\frac{V_{pv} + I_{pv} R_s}{N_s V_T} \right) - 1 \right) - \left(\frac{V_{pv} + I_{pv} R_s}{R_{sh}} \right), \quad (1)$$

where V_T is equal to $(a.k.T/q)$.

The PV panel electrical parameters shown in equation (1) are reported in Table 1.

Table 2 lists the BP SX150S solar panel from BP solar, which is reported at the Standard Test Condition (STC, i.e., 25°C and 1000 W/m^2).

2.2. Boost Power Converter. The boost power converter is inserted between the PV panel and the load as an impedance-matching stage. The PV output voltage (V_{pv}) is regulated to keep it at the nominal voltage (V_{MPP}) by means of an MPPT controller. Voltage regulation is equivalent to controlling the opening and closing of the IGBT power switch through a pulse width modulation (PWM) technology. The IGBT switching frequency is 8 kHz.

To get the most power out of the PV panel that is now available, a new duty ratio D of the PWM signal must be generated in real-time. Table 3 lists the parameter values for the boost converter that was designed. The mathematical equation of the boost converter's output voltage and current has been given as follows [30]:

$$\begin{cases} V_o = \frac{1}{1-D} V_i, \\ I_o = (1-D) I_i, \end{cases} \quad (2)$$

where V_o and I_o are the output's voltages and currents of boost converters, respectively, and V_i and I_i are the input's voltages and currents of boost converters, respectively.

3. Fuzzy MPPT Controller

The fuzzy MPPT controller is an intelligent method of tracking a PV system's maximum power point. In lieu of a precise mathematical model, it uses the fuzzy set theory. The internal functioning of a fuzzy controller of the Mamdani type is based on the structure presented in Figure 2, which includes four blocks [31].

The fuzzification consists in calculating, for each real input value, the degrees of membership to the associated fuzzy sets predefined in the database of the fuzzy system. This block carries out the transformation of the real inputs into symbolic information that can be used by the inference mechanism.

The inference mechanism consists, on the one hand, in calculating the degree of truth of the different rules of the system and, on the other hand, in associating an output value to each of these rules. This output value depends on the conclusion part of the rules, which can take several forms. It can be a fuzzy proposition, and we will speak of a rule of type Mamdani "IF-THEN" in this case:

$$\text{IF } (\dots) \text{ THEN } Y \text{ is } X, \quad X \text{ is set flou.} \quad (3)$$

The defuzzification consists in replacing the set of output values of the various rules resulting from the inference by a single real value representative of this set.

The inputs and outputs of the FLC controller are represented by the triangular and trapezoidal MFs. In Table 4, the letters P and N stand for positive and negative linguistic

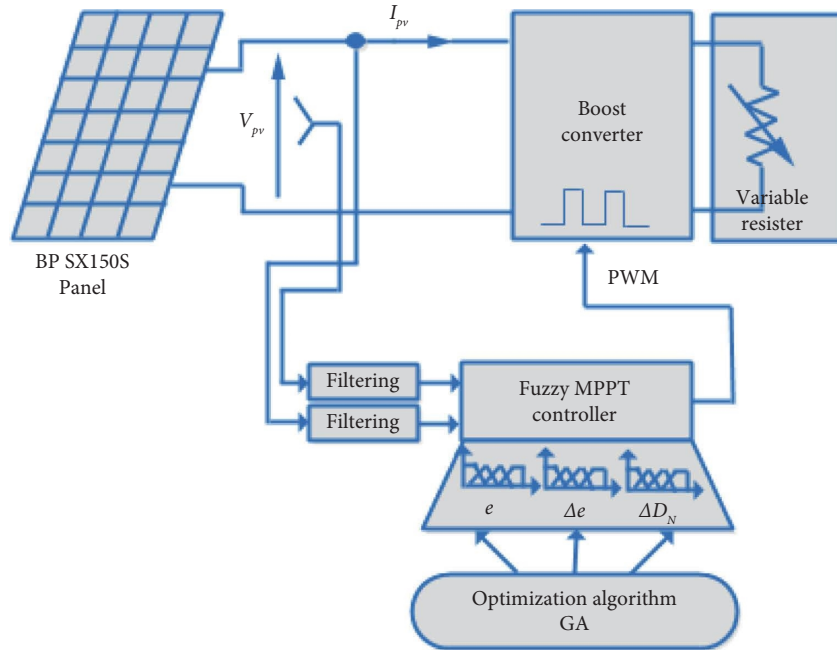


FIGURE 1: The illustrative diagram of the implemented PV system.

TABLE 1: PV panel electrical parameters.

Parameters	Designations
V_T	Diode thermal voltage
a	Diode ideality factor
K	Boltzmann constant
T	Cell's temperature
Q	Electron charge
I_{ph}	Light generated current
I_s	Diode saturation current
R_s	Series equivalent resistances
R_{sh}	Parallel equivalent resistances

variables, respectively. The letters B, S, and ZE additionally stand for Big, Small, and Zero. Five separate linguistic variables are allocated to each input variable, $e(k)$ and $e(k)$. As a result, there are 25 different fuzzy rules in the suggested set of fuzzy rules. The entire set of fuzzy rules is presented in Table 4 [31].

The two input variables that are characterized by the following expressions at a sampling instant k are the error equation (4) and error variation equation (5):

$$e(k) = \frac{P_{pv}(k) - P_{pv}(k-1)}{V_{pv}(k) - V_{pv}(k-1)}, \quad (4)$$

$$\Delta e(k) = e(k) - e(k-1). \quad (5)$$

Based on these two inputs, the FLC calculates the subsequent operating point using MFs and a rule table. The operating point will be on the right or left side of the MPP, depending on whether E is positive or negative. When E equals zero, the MPP is reached. The operational point moves in the MPP direction according to the e-input.

The duty ratio D is computed as follows:

TABLE 2: The BP SX150S solar panel.

Parameters	
Nominal power (P_{MPP})	150 W
Output power tolerance	$\pm 5\%$
Nominal current (I_{MPP})	4.35 A
Nominal voltage (V_{MPP})	34.5 V
Open circuit voltage (V_{oc})	43.5 V
Short circuit current (I_{sc})	4.75 A
Cells number in series (N_s)	72

TABLE 3: DC-DC boost converter specifications.

Electrical specifications	
Inductor (L)	0.6 mH
Input capacitor (C_i)	500 μ F
Output capacitor (C_o)	2200 μ F
Switching frequency (f_s)	8 kHz
IGBT	SKM50GB12T4

$$D(k) = G_D \times \Delta D_N(k) + D(k-1), \quad (6)$$

where ΔD_N is the duty ratio at the controller output and G_D represents the factor's scaling output.

4. Proposed Optimized Fuzzy-Based MPPT

Generally speaking, the following steps can be used to define the genetic algorithm.

4.1. Procedure Genetic Algorithm

Step 1 (initialization). Generate an initial population Pop (t) of size N of chromosomes in a random manner.

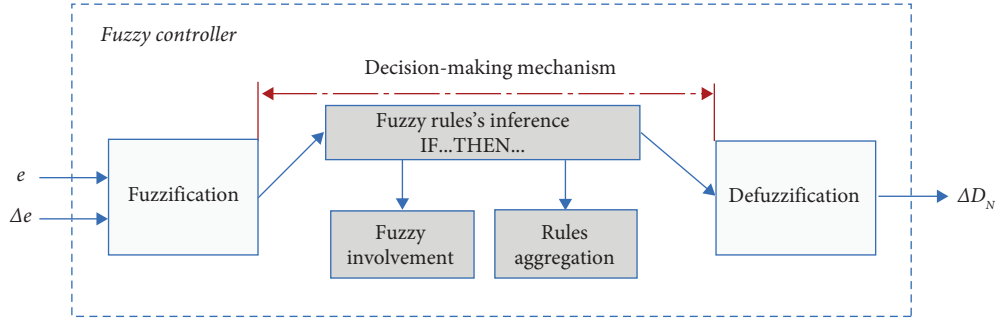


FIGURE 2: The synoptic diagram of a fuzzy controller.

TABLE 4: The rule base table for the fuzzy MPPT controller.

e	Δe				
	NB	NS	ZE	PS	PB
NB	ZE	ZE	PB	PB	PB
NS	ZE	ZE	PS	PS	PS
ZE	PS	ZE	ZE	ZE	NS
PS	NS	NS	NS	ZE	ZE
PB	NB	NB	NB	ZE	ZE

Step 2 (evaluation). Each chromosome is decoded and evaluated Pop (t).

Step 3 (Selection). Production of a new population of N chromosomes with the use of a suitable selection technique, select Pop (t) from Pop ($t-1$).

Step 4 (recombination). According to their probability, crossover, and mutation of some chromosomes within the new population.

Step 5 (termination). To phase 2, as long as the problem stop condition is not satisfied.

4.2. Structure of Chromosomes. In this paper, the membership functions of the fuzzy MPPT controller are optimized. The inputs and output membership functions are each defined by five parameters. For a fuzzy controller with two input variables and one output variable, the membership function numbers are in order 3×5 . Therefore, the GA chromosome's structure is given as a vector of fifteen parameter values, as shown in Figure 3.

4.3. Initial Population. The chromosomes of the original population are set to random variables. A sequence of random numbers $r_{i,j}$ between 0 and 1 is created for each element $X_{i,j}$ of particle i . Then, by projecting $[0, 1]$ into $[X_j^L, X_j^U]$, $X_{i,j}$ is determined as follows:

$$X_{i,j} = X_j^L + r_{i,j} \times (X_j^U - X_j^L), \quad (7)$$

where X_j^L represents the inferior limit of $X_{i,j}$ and X_j^U represents the upper limit of $X_{i,j}$.

4.4. Optimization Criterion. The goal of designing a fuzzy MPPT controller is to discover the optimal settings that minimize energy loss in the PV system, which is mostly caused by meteorological conditions. The optimization criterion's objective function given in equation (8) describes an integral squared error (ISE) function. At each learning step, an ISE value is calculated, and at the end, the best value is returned.

$$ISE = \int_0^{t_f} (e(t))^2 dt, \quad (8)$$

where $e(t) = P_{\max}(t) - P_{pv}(t)$, P_{\max} is the PV panel's rated power, P_{pv} is the PV panel's instant power, and t_f is the simulation time.

4.5. Selection Process. The selection process is applied to the chromosomes of the algorithm. This process is the first step in the selection of the best chromosomes suitable for replication. The tournament selection is used in this work. This selection technique uses proportional selection on chromosome's pairs and then chooses from these pairs the chromosome with the best adaptation (fitness) score.

4.6. Crossover and Mutation Operators. In this study, for a real-coded genetic algorithm, the Laplace crossover operator is suggested [32, 33]. For the real string, a real value mutation has been created. Each parameter $X_{i,j}$ receives an addition of a random with the probability rate pm. The direct application of this mutation can create new parameters outside the interval $[X_j^L, X_j^U]$. Therefore, we propose the following mutation equation (9) for keeping parameters in their range of variation:

$$X_{i,j} = \begin{cases} X_{i,j} + \text{rand}_1 \times (X_j^U - X_{i,j}) & \text{if } \text{rand}_3 < 0.5, \\ X_{i,j} + \text{rand}_2 \times (X_j^L - X_{i,j}) & \text{if } \text{rand}_3 \geq 0.5, \end{cases} \quad (9)$$

where rand_1 , rand_2 , and rand_3 are random numbers between $[0, 1]$.

5. Experimental Results and Discussion

The experimental test bench for the simulated PV system is depicted in Figure 4. The GREAH laboratory in France is where the hardware implementation was developed. The implementation in real time of the proposed MPPT

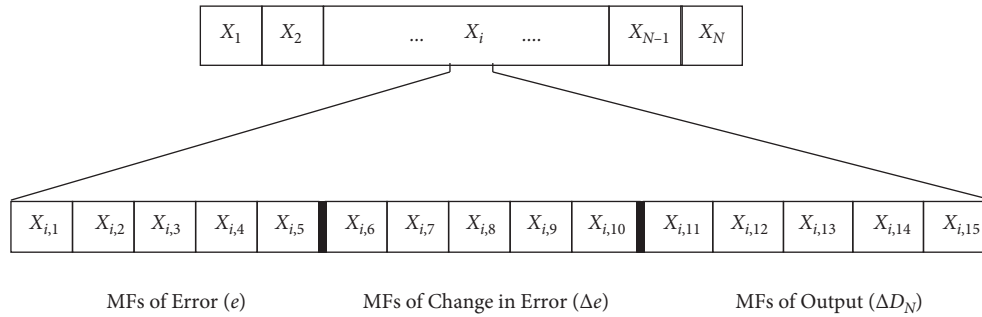


FIGURE 3: The N chromosome's real coding structure.

controller has been given by a dSPACE DS1104 board. The Simulink model of the PV panel as well as the solar radiation and temperature profiles were implemented on a Dspace 1104 board. The reference current and voltage signals computed by the panel control an adjustable DC power supply. Figure 5(a) shows the acquisition chain of the PV source emulator (EPVS). The emulated system involves the use of a boost converter to connect an EPVS to a variable DC load, and the boost's converter specs are illustrated in Table 3. The block for generating PWM signals from the duty ratio values is given in Figure 5(b). The two sensors for measuring voltage and current are Cleqee A622 and TA057, respectively. The sensors have been connected to the dSPACE acquisition board through the ADC ports. The measurements of the sensors have been filtered with digital filters implemented on the dSPACE board, as can be seen through Figure 5(a). The experimental results in Figure 6 have been given at a varying load profile. The load variation was controlled from a dSPACE signal. Figure 5(a) shows the blocks providing the load variation. The observed voltage and current signals are rescaled using gain scales of 10 and 20, respectively. The sample step time in this study is set to $50 \mu s$.

Elgar 5500, a programmable DC power supply, has been used to emulate the electrical characteristics of the PV panel. With the help of this panel emulation, it is possible to make up for the absence of the PV panel and simulate variations in the different profiles. A dSPACE DS1104 controller with a $50 \mu s$ sample period is utilized to create the PV panel Simulink model. The boost converter is controlled by the last via PWM signals with an 8 kHz switching frequency. A DAC output is used to create the analog signal (0-10 V range) needed to command the Elgar 5500 source. The practical properties of the EPVS, as determined by adjusting the power DC supply's output current, are shown in Figure 7

5.1. Optimized Fuzzy MPPT Controller Using dSPACE Implementation. As discussed in the introduction, the reason for implementing the fuzzy MPPT approach is to verify the proposed algorithm experimentally using a dSPACE control board. The fuzzy MPPT controller is computed and optimized under Matlab/Simulink. The control system is set up in accordance with the configuration described in Section 3.

Five membership functions are used to calculate the output variable (ΔD_N) for the FLC as well as the input variables (e and Δe). The variation's ranges for Δe , e , and the output are $[-50, 50]$, $[-35, 5]$, and $[-1.5, 1]$, respectively.

The dSPACE board is the appropriate hardware prototyping improvement solution for doing real-time simulations in many domains and prototyping high-speed digital controllers. These controllers use the MATLAB real-time interfacing toolbox to connect the SIMULINK model to the actual hardware models. Control desk software is used as an acquisition management tool to facilitate real-time analysis of system performance and visualization of PV output waveforms. It is simple to adjust the controller's settings, manage the output load, or change the PV panel's model's mimicked weather patterns using the control desk software. The obtained currents and voltages may also be easily stored and displayed. The main points in the fuzzy MPPT-GA designing in this article are as follows:

- (1) GA learning algorithm
- (2) Experimental testing results

5.1.1. GA's Learning Profile. It is important to note that the optimal parameters of the fuzzy MPPT controller obtained by the GA are strongly related to the adopted methodology. The richer the learning profile and the more real variations in atmospheric conditions are taken into account, the higher the performance of the GA should be. At each step of the algorithm, we have to compromise between exploring the search space to avoid stagnating in a local optimum and exploiting the best individuals obtained to reach better values in the surroundings. If the individuals of a population are too similar, the following populations may become more and more homogeneous. In this case, the evolution of a population may be reduced to the evolution of a single dominant individual, thus reducing the exploration of the search space (premature convergence). In order to be able to efficiently search, it is, therefore, required to maintain a balance between the exploitation of the good solutions encountered and the exploration of unknown areas. An excess of exploitation can lead to a premature convergence (boggling down in a local optimum), just as an excess of exploration could lead to a quasi-random search (no convergence).

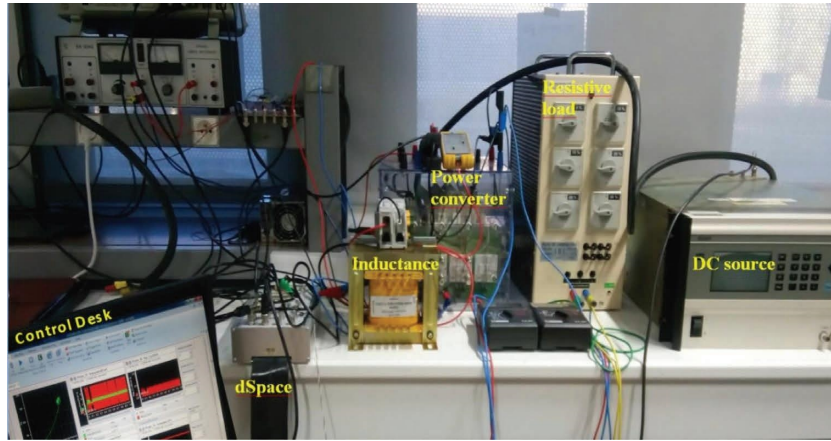


FIGURE 4: The experimental real-time platform.

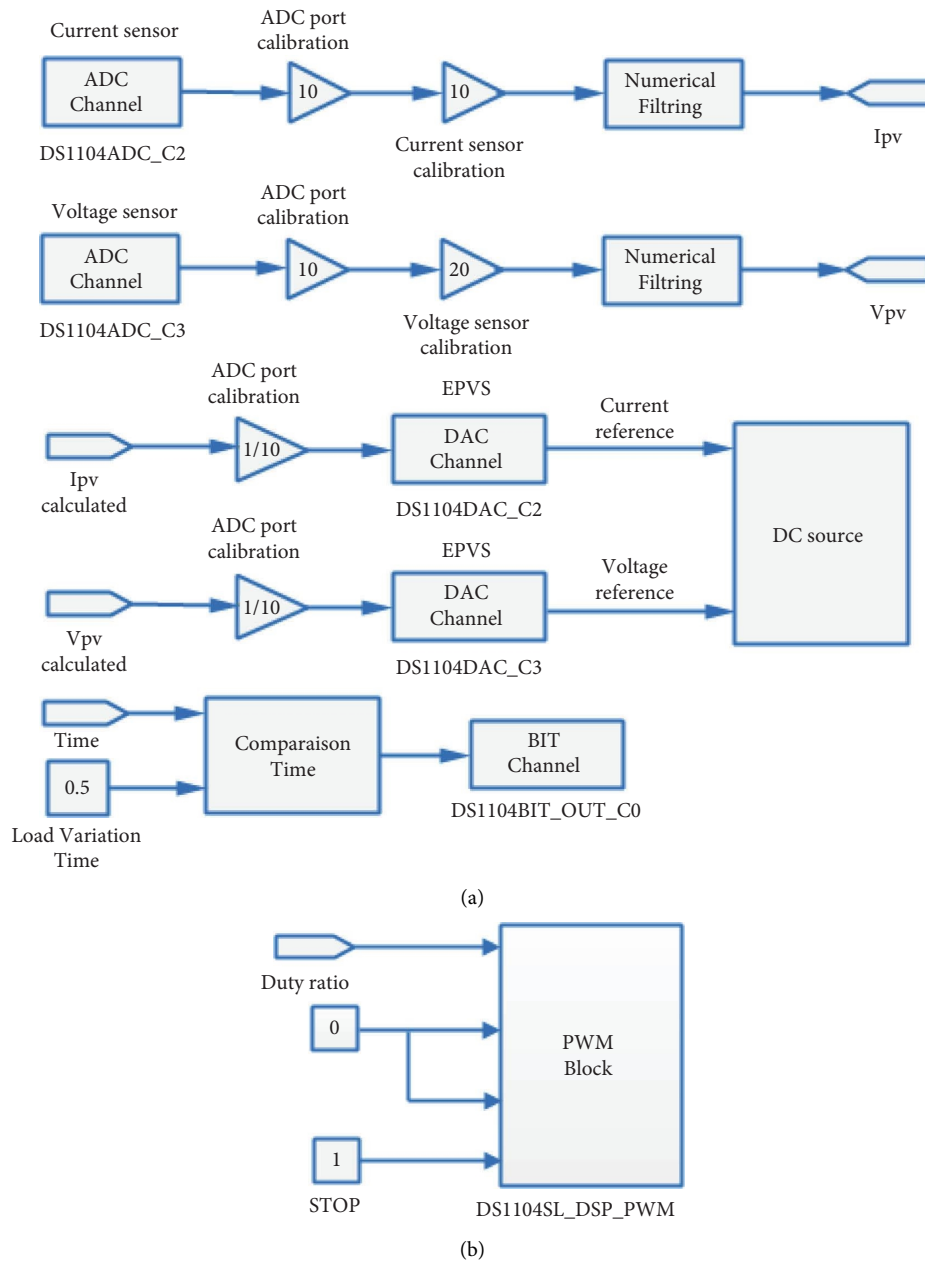


FIGURE 5: (a) ADC and DAC conversion blocks and (b) the PWM block.

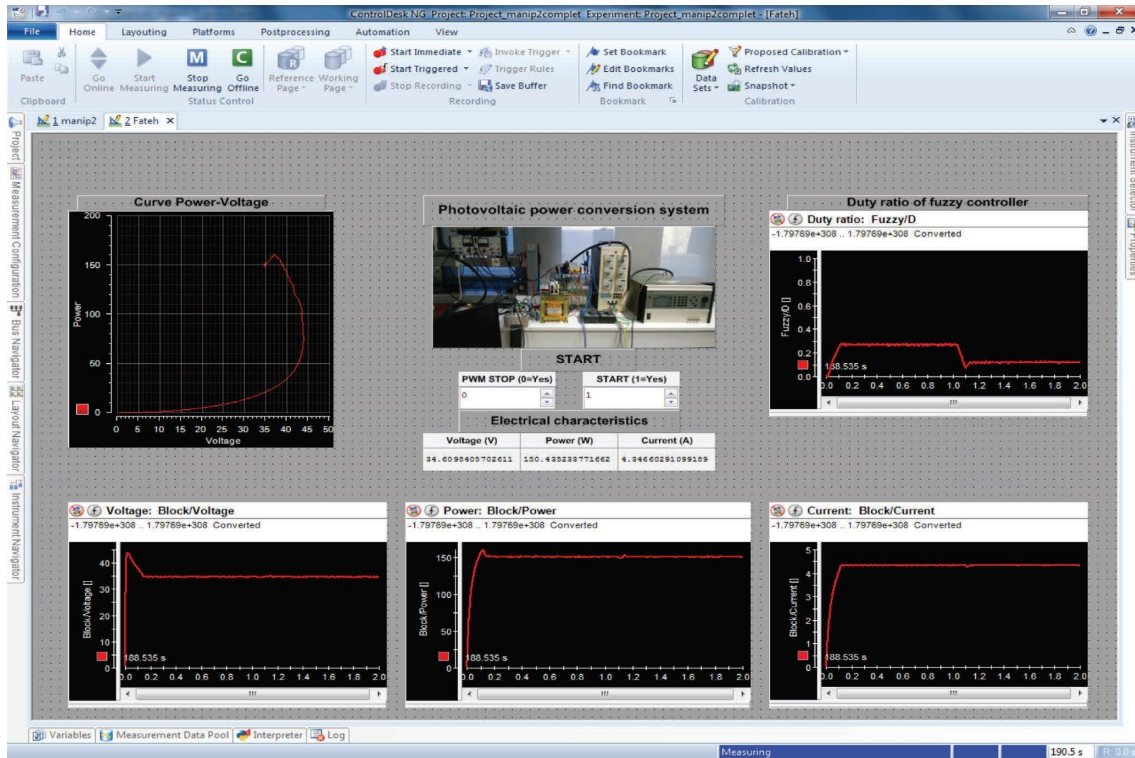


FIGURE 6: The control desk interface of the EPVS system.

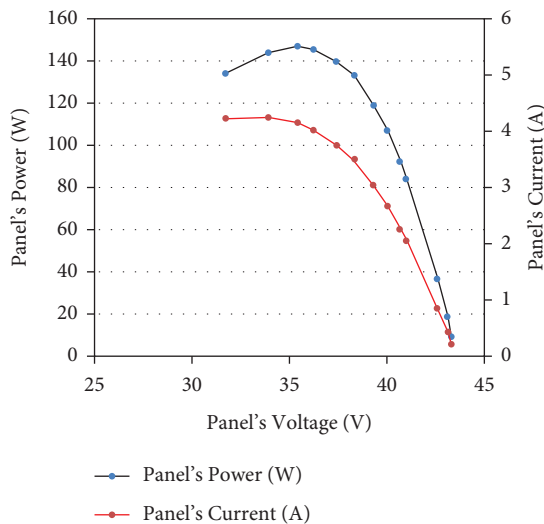


FIGURE 7: EPVS's experimental electrical characteristics.

The learning profile of the GA adopted is important for an optimal parameter result and must include any scenario that the system may encounter in the irradiance variations and from the values returned by the objective function ISE. A selection of the best chromosome (individuals) has been made by the algorithm. For this purpose, the parameters of the best chromosome were introduced to the fuzzy MPPT controller.

The value in the learning profile begins at 600 W/m^2 and changes at 1100 W/m^2 after 2 s; this value is maintained until 4 s after another change occurs to reach the value of 800 W/m^2 .

The simulation results are given at a population of 20 chromosomes, and the training of the algorithm has been given at 200 iterations. The values of the fitness function ISE evolve in a decreasing way from iteration 01 to iteration 50. Beyond this iteration, the evolution of the curve is constant until it reaches the value ISE 0.372. The fact of training the algorithm beyond 50 iterations tells us that the algorithm has found a global optimum. The evolution of the ISE function curve per iteration is shown in Figure 8.

5.1.2. Experiments Testing Results. After the learning process is accomplished, we can see the tracking performance corresponding to the optimal solution obtained by the GA. The experimental testing results are obtained using the following two scenarios. The studied EPVS system has been evaluated in a 2 s total duration with a $50 \mu\text{s}$ fixed step size during the testing phases.

- (i) In the first test, the solar irradiance and temperature are kept constant at STC conditions, but an instantaneous load change is performed at 1s. The resistance goes from a value of 20Ω to 14Ω .
- (ii) In the second test, the load is kept constant at $R = 20 \Omega$. However, the goal of this test is to study the impact of the fast-changing of solar irradiance on the performance of the proposed MPPT algorithm.

(1) *Performance Test at Standard Conditions and Fast Varying Load Conditions.* An interface controls the

parameters of the experimental test bench of the EPVS system and thus displays the curves and results of the electrical characteristics. The control of parameters is given by two buttons: START and PWM STOP. In order to activate the control part, the START value is set to 1, and the PWM STOP value is set to 0. The values of the electrical characteristics represented are voltage (V), power (W), and current (A). The curves shown are the power-voltage curve, the duty cycle of the proposed controller, and thus the voltage, power, and current.

The results represented in this interface have been given for a temperature of 25°C and sunshine 1000 W/m² as well as a fast-varying resistance load. Figure 6 shows the control desk interface of the EPVS system.

Figures 6 and 9 show the results of the generated EPVS power of the proposed fuzzy MPPT-GA. In the presented results, during the transient load step of $R = 20 \Omega$ between 0 s and 0.5 s, it can be seen that the proposed fuzzy MPPT-GA converges rapidly to the MPP at a time of 0.08 s with a tracking error of 3% and a steady state-error of 99.87% and then the power is maintained around 150 W with an extremely low steady-state error of about $\pm 0.13\%$. The total error between the tracking error and the steady-state error is about 96.87%.

In the second transient load step of $R = 14 \Omega$ between 0.5 s and 1 s, it is clearly observed that the proposed fuzzy MPPT-GA shows better power generation, which much perfectly rated around 150 W with an extremely low steady-state error of about $\pm 0.13\%$ (99.87%) as depicted in Figures 6 and 9. It can be concluded that the proposed fuzzy MPPT-GA completely follows the maximum power of 150 W to the STC test profile and also to the fast-varying load conditions.

Figure 10 shows the result of the duty ratio of the proposed fuzzy MPPT-GA at the STC. It can be observed a variation in the duty ratio value as soon as 0.5 s. In the presented results, during the transient load step of $R = 20 \Omega$ between 0 s and 0.5 s, it can be seen that the proposed fuzzy MPPT-GA generates a duty ratio of the value $D = 0.25$. It is evident that the proposed fuzzy MPPT-GA generates the corresponding new duty ratio D ($D = 0.15$) for each transaction period in the second transient load level of $R = 14 \Omega$ between 1 s and 2 s, which establishes the new position of the desired MPP inversely. In this case, the duty ratio of the proposed fuzzy MPPT-GA is optimally adjusted. It is clearly shown that a perfect duty ratio is generated in order to keep the power produced at its desired value.

(2) *Performance Test under Fast-Changing Solar Irradiation.* The test at standard conditions, as well as at the fast variation of the load, has been successfully performed. Now, a test at fast variation solar irradiation has been performed. The load was held fixed at $R = 20 \Omega$. The choice of the value between $R = 20 \Omega$ or $R = 14 \Omega$ is not important since the result given in Figures 6 and 9 clearly shows that the power is maintained at 150 W with an error of 0.13% at the static regime for both the resistance values.

Figure 11 shows the irradiance profile, which varies between 1000 W/m² and 1100 W/m², and both the

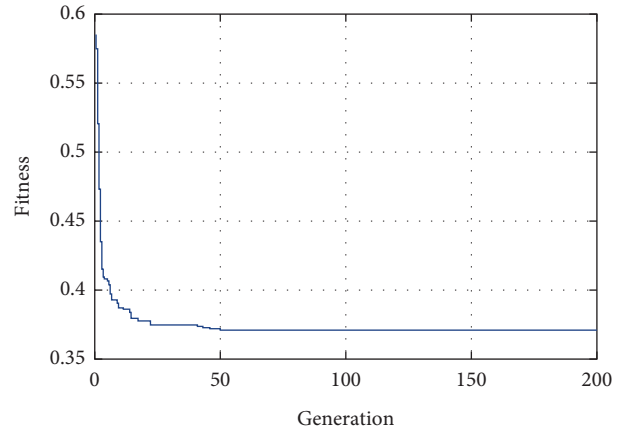


FIGURE 8: Evolution of the fitness function curve.

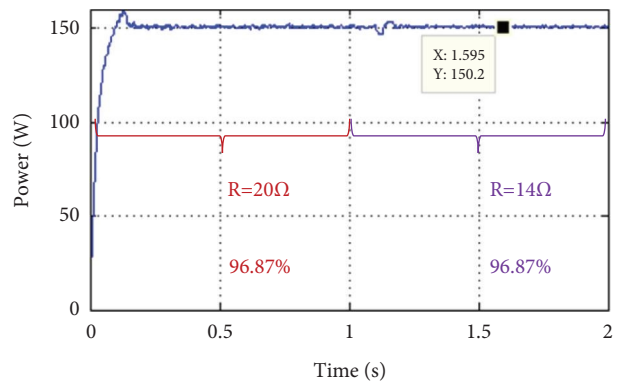


FIGURE 9: The experimental result of PV power under STC and fast-varying load.

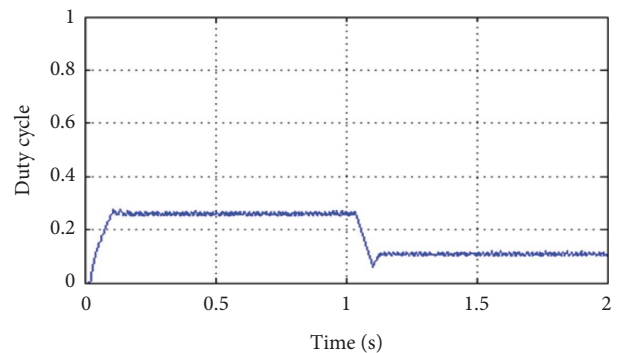


FIGURE 10: The experimental result of the duty ratio ΔD_N under STC and fast-varying load.

temperature and the load charge are kept constant during the experiments at 25°C and $R = 20 \Omega$, respectively.

The experimental performance test has been carried out at the fixed charge 20Ω and the fast-changing solar irradiance, as shown in Figure 11. In this test case, the objective has been to evaluate and observe the response of the proposed fuzzy MPPT-GA only to the fast-changing solar irradiance and at the constant ambient temperature 25°C.

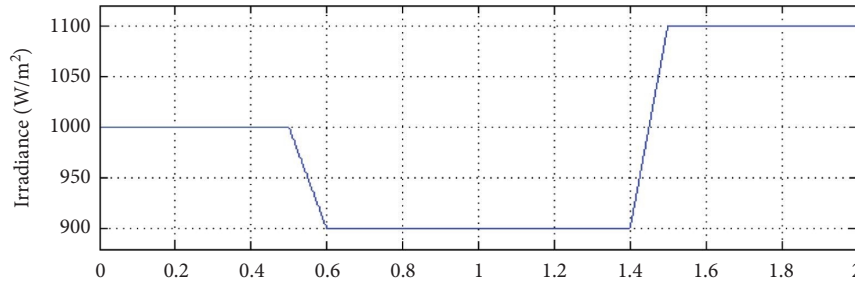


FIGURE 11: The irradiance profile.

Figure 12 shows the results of the generated EPVS power of the proposed fuzzy MPPT-GA. In the presented results, during the transient irradiance value between 0 s and 0.5 s, it can be seen that the proposed fuzzy MPPT-GA converges very rapidly to the MPP at a time of 0.06 s with a tracking error of 2.6% and a steady-state error of 99.85% and then the power is maintained around 150 W for a 1000 W/m² with an extremely low steady-state error of about $\pm 0.10\%$. The total error between the tracking error and the steady-state error is about 97.25%. In the second step, the transient irradiance value is between 0.5 s and 1.4 s. It can be seen that the proposed fuzzy MPPT-GA also converges at the MPP with an extremely low steady-state error of about $\pm 0.12\%$ (99.82%). In the last step, during the transient period of 1.4 s to 2 s, it can be seen that the proposed fuzzy MPPT-GA also converges at the MPP with an extremely low steady-state error of about $\pm 0.14\%$ (99.79%). The efficiency of the EPVS system in the three transient irradiance values has been given at 98.95%. It can be clearly observed that the result, when the MPP abruptly changes, is that the proposed fuzzy MPPT-GA may immediately push the EPVS system to the new MPP.

Figure 13 shows the result of the duty ratio of the proposed fuzzy MPPT-GA under fast-changing solar irradiation. It can be clearly observed that a new value of the duty cycle has been generated at each variation of the irradiance. In this case, the duty ratio of the proposed fuzzy MPPT-GA has been optimally adjusted in order to keep the operating point at each instant at the MPP.

Now, the proposed fuzzy MPPT-GA has been compared with a few strategies which have been published in recent works to optimize FLC-based MPPT meths. Authors in [18, 24, and 25] have performed the performance tests of standalone PV systems only at STC conditions with a fixed resistance load. The results of tests for a profile of variable irradiance that present overshoots when changing the values of irradiance more or less different from one paper to another have been presented in [18, 19, and 21].

For a more logical comparison, the optimization algorithms should use the same objective function (equation (7)), the same initial population, and also the same number of iterations. The advantages of our design strategy, which provides the best objective function (ISE) value at the conclusion of the optimization process, have been shown in Figure 8.

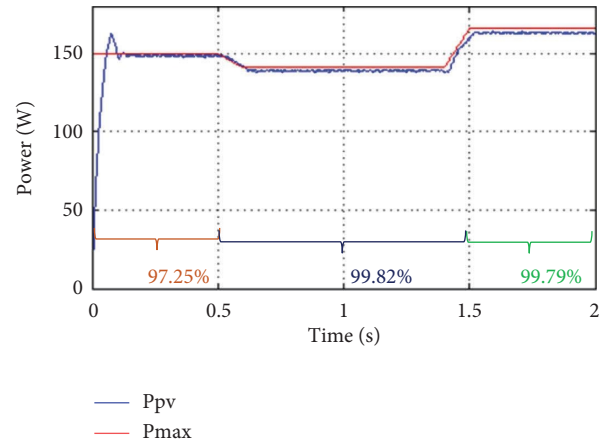
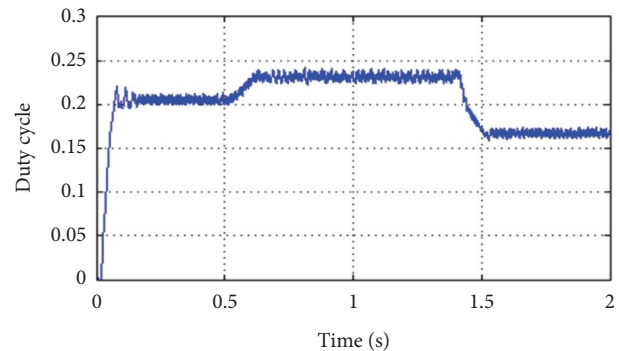


FIGURE 12: The experimental result of PV power under fast-changing solar irradiation.

FIGURE 13: The experimental result of the duty ratio ΔD_N under fast-changing solar irradiation.

6. Conclusion

This paper presents a modeling and experimental validation of a standalone PV system. The system under investigation consists of a DC power source that simulates a solar panel, a DC/DC boost converter, a resistive load, and a real-time maximum power point tracking controller integrated into a dSPACE DS1104 board. The GA has been successfully applied in this study to optimize the productivity of a fuzzy MPPT algorithm by improving the controller's membership function parameters. From the objective function values obtained in the simulation, it is seen that the GA provides

a good approach for designing efficient fuzzy MPPT. The following are the main highlights of the current work:

- (i) The proposed GA algorithm's learning profile was extremely important. The results obtained during the tests using the various profiles clearly show that the parameters of the fuzzy controller's input/output membership functions determined during the optimization process accurately follow the GMPP with a steady-state error of around $\pm 0.13\%$.
- (ii) Similar to that, a reference signal has been used to compare the proposed approach. The outcomes demonstrated the suggested algorithm's capability to track the GMPP with quicker convergence and fewer power fluctuations than before. The suggested fuzzy controller optimized-based MPPT's viability and efficacy have been tested experimentally, and the findings unmistakably show that it is capable of tracking the GMPP with an average efficiency of 98.66% and an average tracking time of 0.08 s and 0.06 s under the STC and the fast-changing solar irradiance, respectively.

The outcomes demonstrated that the suggested approach was workable and that it was capable of tracking the maximal power point with high efficiency that exceeded 97.8% in all tested scenarios. The method proposed has been described in some detail and can be used in other similar systems.

Data Availability

The data supporting the findings of the current study are available from the corresponding author upon request.

Conflicts of Interest

The authors declare that they have no conflicts of interest.

References

- [1] S. S. Kshatri, J. Dhillon, S. Mishra et al., "Reliability analysis of bifacial PV panel-based inverters considering the effect of geographical location," *Energies*, vol. 15, p. 170, 2021.
- [2] M. U. Siddiqui, O. K. Siddiqui, A. B. Alqaity, H. Ali, A. F. M. Arif, and S. M. Zubair, "A Comprehensive Review on Multi-Physics Modeling of Photovoltaic Modules," *Energy Conversion and Management*, Article ID 115414, 2022.
- [3] N. M. Kumar, S. Islam, A. K. Podder, A. Selim, M. Bajaj, and S. Kamel, "Lifecycle-based feasibility indicators for floating solar photovoltaic plants along with implementable energy enhancement strategies and framework-driven assessment approaches leading to advancements in the simulation tool," *Frontiers in Energy Research*, vol. 11, 2023.
- [4] C. Aoughlis, A. Belkaid, I. Colak, O. Guenounou, and M. A. Kacimi, "Automatic and self-adaptive P&O MPPT based PID controller and PSO algorithm," in *Proceedings of the 2021 10th International Conference on Renewable Energy Research and Application (ICRERA)*, pp. 385–390, IEEE, Istanbul, Turkey, September 2021.
- [5] R. Kumar, S. Khandelwal, P. Upadhyay, and S. Pulipaka, "Global maximum power point tracking using variable sampling time and pv curve region shifting technique along with incremental conductance for partially shaded photovoltaic systems," *Solar Energy*, vol. 189, pp. 151–178, 2019.
- [6] F. Zaouche, D. Rekioua, J. P. Gaubert, and Z. Mokrani, "Supervision and control strategy for photovoltaic generators with battery storage," *International Journal of Hydrogen Energy*, vol. 42, no. 30, pp. 19536–19555, 2017.
- [7] M. Sarvi and A. Azadian, "A comprehensive review and classified comparison of MPPT algorithms in PV systems," *Energy Systems*, vol. 13, no. 2, pp. 281–320, 2021.
- [8] F. Yahiaoui, F. Chabour, O. Guenounou et al., "Experimental validation and intelligent control of a stand-alone solar energy conversion system using dSPACE platform," *Frontiers in Energy Research*, vol. 10, 2022.
- [9] D. Rekioua, F. Zaouche, H. Hassani, T. Rekioua, and S. Bacha, "Modeling and fuzzy logic control of a stand-alone photovoltaic system with battery storage," *Turkish Journal of Electromechanics and Energy*, vol. 4, no. 1, 2019.
- [10] A. Boudia, S. Messalti, A. Harrag, and M. Boukhniher, "New hybrid photovoltaic system connected to superconducting magnetic energy storage controlled by PID-fuzzy controller," *Energy Conversion and Management*, vol. 244, Article ID 114435, 2021.
- [11] C. Balasundar, S. Ck, S. Ns, and J. M. Guerrero, "Interval type-II fuzzy logic controlled shunt converter coupled novel high-quality charging scheme for electric vehicles," *IEEE Transactions on Industrial Informatics*, 2020.
- [12] A. Mohammadzadeh, M. H. Sabzalian, and W. Zhang, "An interval type-3 fuzzy system and a new online fractional-order learning algorithm: theory and practice," *IEEE Transactions on Fuzzy Systems*, vol. 28, no. 9, pp. 1940–1950, 2020.
- [13] D. S. Abraham, B. Chandrasekar, N. Rajamanickam et al., "Fuzzy-based efficient control of DC microgrid configuration for PV-energized EV charging station," *Energies*, vol. 16, no. 6, p. 2753, 2023.
- [14] A. Jaiswal, Y. Belkhier, S. Chandra et al., "Design and implementation of energy reshaping based fuzzy logic control for optimal power extraction of PMSG wind energy converter," *Frontiers in Energy Research*, vol. 10, 2022.
- [15] S. B. Hamed, A. Abid, M. B. Hamed et al., "A robust MPPT approach based on first-order sliding mode for triple-junction photovoltaic power system supplying electric vehicle," *Energy Reports*, vol. 9, no. 2023, pp. 4275–4297, 2023.
- [16] D. E. Goldenberg, "Genetic Algorithms in Search," *Optimization and Machine Learning*, 1989.
- [17] A. Hadjaissa, S. Ait cheikh, K. Ameur, and N. Essounbouli, "A GA-based optimization of a fuzzy-based MPPT controller for a photovoltaic pumping system, Case study for Laghouat, Algeria," *IFAC-PapersOnLine*, vol. 49, no. 12, pp. 692–697, 2016.
- [18] A. Borni, T. Abdelkrim, N. Bouarroudj et al., "Optimized MPPT controllers using GA for grid connected photovoltaic systems, comparative study," *Energy Procedia*, vol. 119, pp. 278–296, 2017.
- [19] O. Guenounou, A. Belkaid, I. Colak, B. Dahhou, and F. Chabour, "Optimization of fuzzy logic controller based maximum power point tracking using hierarchical genetic algorithms," in *Proceedings of the 2021 9th International Conference on Smart Grid (icSmartGrid)*, pp. 207–211, IEEE, Setubal, Portugal, June 2021.
- [20] K. Loukil, H. Abbes, H. Abid, M. Abid, and A. Toumi, "Design and implementation of reconfigurable MPPT fuzzy controller for photovoltaic systems," *Ain Shams Engineering Journal*, vol. 11, no. 2, pp. 319–328, 2020.

- [21] A. Messai, A. Mellit, A. Guessoum, and S. A. Kalogirou, "Maximum power point tracking using a GA optimized fuzzy logic controller and its FPGA implementation," *Solar Energy*, vol. 85, no. 2, pp. 265–277, 2011.
- [22] C. N. S. Kalyan, B. S. Goud, M. Bajaj, M. K. Kumar, E. M. Ahmed, and S. Kamel, "Water-cycle-algorithm-tuned intelligent fuzzy controller for stability of multi-area multi-fuel power system with time delays," *Mathematics*, vol. 10, no. 3, p. 508, 2022.
- [23] A. Youssef, M. E. Telbany, and A. Zekry, "Reconfigurable generic FPGA implementation of fuzzy logic controller for MPPT of PV systems," *Renewable and Sustainable Energy Reviews*, vol. 82, pp. 1313–1319, 2018.
- [24] A. Ilyas, M. R. Khan, and M. Ayyub, "FPGA based real-time implementation of fuzzy logic controller for maximum power point tracking of solar photovoltaic system," *Optik*, vol. 213, Article ID 164668, 2020.
- [25] S. Hadji, J. P. Gaubert, and F. Krim, "Real-time genetic algorithms-based MPPT: study and comparison (theoretical an experimental) with conventional methods," *Energies*, vol. 11, no. 2, p. 459, 2018.
- [26] D. Fares, M. Fathi, I. Shams, and S. Mekhilef, "A novel global MPPT technique based on squirrel search algorithm for PV module under partial shading conditions," *Energy Conversion and Management*, vol. 230, Article ID 113773, 2021.
- [27] I. Shams, S. Mekhilef, and K. S. Tey, "Maximum power point tracking using modified butterfly optimization algorithm for partial shading, uniform shading, and fast varying load conditions," *IEEE Transactions on Power Electronics*, vol. 36, no. 5, pp. 5569–5581, 2021.
- [28] M. B. Yaouba, M. Bajaj, C. Welba et al., "An experimental and case study on the evaluation of the partial shading impact on PV module performance operating under the sudano-sahelian climate of Cameroon," *Frontiers in Energy Research*, vol. 10, 2022.
- [29] R. Khelifi, M. Guermoui, A. Rabehi et al., "Short-term PV power forecasting using a hybrid TVF-EMD-ELM strategy," *International Transactions on Electrical Energy Systems*, vol. 2023, Article ID 6413716, 14 pages, 2023.
- [30] X. Weng, X. Xiao, W. He et al., "Comprehensive comparison and analysis of non-inverting buck boost and conventional buck boost converters," *Journal of Engineering*, vol. 2019, no. 16, pp. 3030–3034, 2019.
- [31] S. Tamalouzt, Y. Belkhier, Y. Sahri, N. Ullah, R. N. Shaw, and M. Bajaj, "New direct reactive power control based fuzzy and modulated hysteresis method for micro-grid applications under real wind speed," *Energy Sources, Part A: Recovery, Utilization, and Environmental Effects*, vol. 44, no. 2, pp. 4862–4887, 2022.
- [32] O. Guenounou, B. Dahhou, and F. Chabour, "TSK fuzzy model with minimal parameters," *Applied Soft Computing*, vol. 30, pp. 748–757, 2015.
- [33] L. Brikh, O. Guenounou, and T. Bakir, "Selection of minimum rules from a fuzzy TSK model using a PSO-fcm combination," *Journal of Control, Automation and Electrical Systems*, vol. 34, no. 2, pp. 384–393, 2022.